Simple *M*-factor algorithm for improved estimation of the basic maximum usable frequency of radio waves reflected from the ionospheric F-region

M. Lockwood, B.Sc., Ph.D.

Indexing term: *Radio-wave propagation*

Abstract: The equations of Milsom are evaluated, giving the ground range and group delay of radio waves propagated via the horizontally stratified model ionosphere proposed by Bradley and Dudeney. Expressions for the ground range which allow for the effects of the underlying E- and F1-regions are used to evaluate the basic maximum usable frequency or *M*-factors for single F-layer hops. An algorithm for the rapid calculation of the *M*-factor at a given range is developed, and shown to be accurate to within 5%. The results reveal that the *M*(3000)F2-factor scaled from vertical-incidence ionograms using the standard URSI procedure can be up to 7.5% in error. A simple addition to the algorithm effects a correction to ionogram values to make these accurate to 0.5%.

1 Introduction

The basic maximum usable frequency (MUF) is defined by the International Radio Consultative Committee (CCIR) as the highest frequency that can propagate between a pair of terminals by ionospheric refraction alone [1]. The MUF can be estimated in one of two ways: first, ray computations can be made for a succession of increasing frequencies until propagation to the required ground range is no longer possible; alternatively, equations based on relationships for mean reference ionospheres can be employed [2]. The advantages of the former iterative procedure are that the effects of spatial variations in the height of the reflecting layer and in the underlying ionospheric regions can be taken into account, and that the evaluation can be continued until the required accuracy is achieved. However, for many applications it is undesirable to have an indeterminate computation time, and the accuracy of the ionospheric data may not justify such a procedure. In these cases the second approach is favoured.

The F2-layer *M*-factor for a ground range D, $M(D)$F2, is defined as the MUF divided by the critical frequency foF2. The value for 3000 km, $M(3000)$F2, is routinely scaled from the ordinary wave trace of ionograms using the standard URSI slider, which neglects the effect of the geomagnetic field [3].

The noniterative procedure recommended by the CCIR for F2-mode MUF evaluation, described in Report 340-4 [4], requires knowledge of values for foF2 $M(3000)$F2 and the gyrofrequency f_H. The MUF for $D=0$ is taken to be (foF2 + $f_H/2$), to allow for the effect of the geomagnetic field, and for $D=4000$ km a value of $1.1\,M(3000)f$oF2 is used. A nomogram or associated computer coding is then used to interpolate to the value for the range D. However, the nomogram only incorporates a mean fixed allowance for the effects of ionisation beneath the F2-layer.

In this paper a noniterative procedure is developed which enables evaluation of the basic MUF using $M(D)$F2, with allowance for variations in both the peak height and changes in the underlying plasma. An algorithm is presented based on values of the ionospheric characteristics foF2, foE and $M(3000)$F2.

Paper 2522F, first received 2nd August 1982 and in revised form 4th January 1983

The author is with the Rutherford Appleton Laboratory, Chilton, Didcot OX11 0QX, England

Use is made of the Bradley-Dudeney model of the electron density profile [5], consisting of a combination of linear and parabolic segments to represent the E-, F1- and F2-regions. However, exact analytic solution of the radiowave ray path is possible for neither of these two profile forms. DeVoogt [6] suggested an approximation to a parabolic form, referred to as a quasiparabolic profile, and full analytic solutions for propagation via this profile have been given by Croft and Hoogasian [7]. Similarly, a quasilinear form was proposed by Muldrew [8], and equations for corresponding ray paths are given by Westover [9]. Milsom [10] has fitted quasi-parabolic and quasilinear segments to give a close approximation to the Bradley-Dudeney profile, thereby allowing rapid calculation of ray-path parameters.

2 Ray-path equations and *M*-factor evaluation procedure

The general form of the Milsom fit to the Bradley-Dudeney model profile is demonstrated by Fig. 1. The ray-path of a single F2 hop, reflected by a horizontally stratified ionosphere

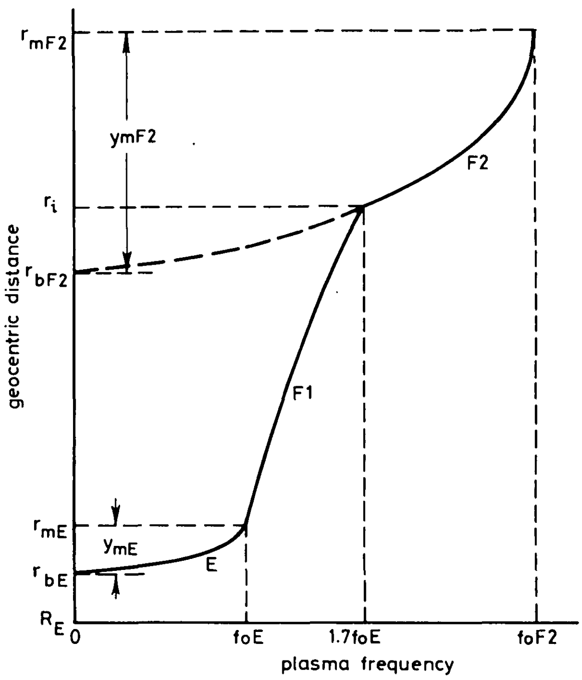

Fig. 1 *Fit of quasiparabolic and quasilinear segments to the Bradley-Dudeney model profile*

with this profile, is shown in Fig. 2. That part of the ray path between geocentric distances r_b and r_t subtends an angle α at the earth's centre, given by Bouger's rule as

$$\alpha = \int_{r_b}^{r_t} \frac{R_E \cos\beta_0}{r(r^2\mu^2(r) - R_E^2\cos^2\beta_0)^{1/2}}\,dr \qquad (1)$$

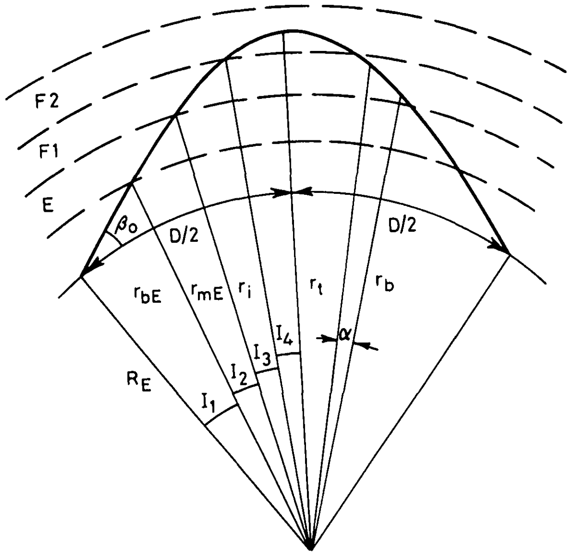

Fig. 2 *Ray path of a single hop reflected from the F2-layer*

where μ is the refractive index for the wave frequency f, and β_0 is the elevation of the ray path at the earth's surface, the radius of curvature of which is R_E. The ground range of the single F2 hop is

$$D = 2R_E(I_1 + I_2 + I_3 + I_4) \qquad (2)$$

where the contribution from each of the model profile segments (I_1, I_2, I_3 and I_4, see Fig. 2) can be calculated from eqn. 1. The adoption of quasilinear and quasiparabolic forms enables analytic solution, neglecting the effects of the magnetic field and electronic collisions [10]:

$$I_1 = (\gamma - \beta_0) \qquad (3)$$

$$I_2 = \frac{R_E\cos\beta_0}{\sqrt{C}}\left[\sinh^{-1}\left\{\frac{Br_{bE} + 2C}{|r_{bE}(4AC - B^2)^{1/2}|}\right\} - \sinh^{-1}\left\{\frac{Br_{mE} + 2C}{|r_{ME}(4AC - B^2)^{1/2}|}\right\}\right] \qquad (4)$$

$$I_3 = \frac{1}{2}\left[\sin^{-1}\left\{\frac{B_1 - 2(r_{bE}\cos\gamma/r_1)^2}{(B_1^2 - 4A_1C_1)^{1/2}}\right\} - \sin^{-1}\left\{\frac{B_1 - 2(r_{bE}\cos\gamma/r_{mE})^2}{(B_1^2 - 4A_1C_1)^{1/2}}\right\}\right] \qquad (5)$$

$$I_4 = \frac{R_E\cos\beta_0}{C_{11}^{1/2}} \times \log_n\left\{\frac{B_{11} + 2C_{11}/r + (A_{11}r_1^2 + B_{11}r_1 + C_{11})^{1/2}(2C_{11}^{1/2}/r_1)}{(B_{11}^2 - 4A_{11}C_{11})^{1/2}}\right\} \qquad (6)$$

where

$$\gamma = \cos^{-1}(R_E\cos\beta_0/r_{bE}) \qquad (7)$$

$$A = 1 - \left\{\frac{f\text{oE}}{f}\right\}^2\left[1 - \left\{\frac{r_{bE}}{y_{mE}}\right\}^2\right] \qquad (8)$$

$$B = -2r_{mE}\left\{\frac{r_{bE}f\text{oE}}{y_{mE}f}\right\}^2 \qquad (9)$$

$$C = \left\{\frac{r_{mE}r_{bE}f\text{oE}}{y_{mE}f}\right\}^2 - R_E^2\cos^2\beta_0 \qquad (10)$$

$$A_1 = \frac{-1.89f\text{oE}^2}{f^2(r_1^2 - r_{mE}^2)} \qquad (11)$$

$$B_1 = 1 - \left\{\frac{f\text{oE}}{f}\right\}^2\left\{1 - \frac{1.89r_{mE}^2}{(r_1^2 - r_{mE}^2)}\right\} \qquad (12)$$

$$C_1 = -R_E^2\cos^2\beta_0 \qquad (13)$$

and A_{11}, B_{11} and C_{11} are given by eqns. 8, 9 and 10, respectively, with the F-region parameters foF2, r_{mF2}, r_{bF2} and ymF2 substituted for their corresponding E-region values.

Eqns. 2–13 enable the ground range D for a wave of frequency f and elevation angle β_0 to be calculated for a given model profile. Note that the contribution of underlying ionospheric regions is accounted for.

For a given f and model profile the minimum value of D, or skip distance, was evaluated iteratively for a range of β_0 within limits to provide F2-layer reflections, determined using Bouger's rule. The frequency is then the basic MUF. The variation of the M-factor (MUF/foF2) with D was obtained by repeating the above procedure for various values of f in the range between foF2 and f_{max}, the frequency which just penetrates the F-layer at zero elevation. The maximum value of M is

$$M_{max} = \frac{f_{max}}{f\text{oF2}} = \left\{1 - \left(\frac{R_E}{R_E + h\text{mF2}}\right)^2\right\}^{-1/2} \qquad (14)$$

The value of f was also iterated to achieve a skip distance of 3000 km (± 0.1 km), giving the M-factor for this range. This value will be referred to as $M(3000)_o$, the subscript denoting its derivation from the equations of oblique propagation. A second value for this factor, scaled from the vertical incidence ionogram using the standard URSI procedure, is discussed in Section 6 and is denoted by $M(3000)_i$.

The rapidity with which the hop length can be computed using eqns. 2–13 enables the achievement of the desired accuracy of the double iteration to the $M(3000)_o$ value in a relatively small amount of computer time. Hence the procedure could easily be repeated for a large number of model profiles.

3 Model parameters adopted

A range of model ionospheres was considered in order to investigate the variation of $M(D)$F2 with range D, and hence to devise an algorithm to determine $M(D)$F2 for given D, $M(3000)_i$, foE and foF2.

In the Bradley-Dudeney model the peak height and semi-thickness of the E-layer are set to 110 and 20 km, respectively. Hence the entire profile is characterised by the remaining four independent variables foF2, foE, ymF2 and hmF2. In this study of M-factors it is necessary to use only one value of

foF2, with various values of x, the ratio (foF2/foE). The number of variables is further reduced to two by adopting a fixed value for the ratio hmF2/ymF2 of 3.5. The real-height analysis by Bradley and Dudeney [5] gave a spread of values for this ratio between 2.0 and 5.5, but for a single parabolic layer such a spread results in a maximum change in the M-factor of about 3%. The Bradley-Dudeney profile is independent of ymF2 if x equals the lower limit of 1.7. Hence this M-factor change tends to zero as x approaches 1.7. The results show that for the case of $x = 10$ and hmF2 = 350 km the above variation in ymF2 caused near-identical changes in $M(3000)_o$ and $M(3000)_i$, and that the corresponding changes in $M(D)$ for different D were always less than 0.5%.

A range of hmF2 between 250 km and 500 km was employed. Occasionally in practice hmF2 can be below 250 km, but it was found that the variation of M-factors with hmF2 was smaller the the lower heights and that six values (50 km apart) were adequate to characterise their behaviour. The M-factor value was found to be very dependent on x near its lower limit of 1.7, but more slowly varying at large x. Hence values equally spaced in $1/x$ were used with some extra low x cases. The x values used were 10, 5, 3.33, 2.5, 2.2, 2.08 and 2.0, giving a total of 42 curves of $M(D)$ which were calculated. For x below 2.0 it was found that F2-layer M-factors depend sensitively on x. Reflection by the F2-layer is then only possible for a small range of the elevation angle β_0, and such propagation is to restricted values of D. In addition M-factor values become more model dependent as x approaches the limit of 1.7. The algorithm presented here is not, therefore, designed for use at x below about 1.95. The greatly increased complexity required to characterise the behaviour of M-factors for any lower x is not justified by the model approximations. Cases of x below 1.95 are rare; low x values are predominantly a feature of the daytime high-latitude ionosphere in winter at sunspot minimum.

4 F-layer M-factors

Fig. 3, giving M-factors as a function of ground range for propagation via model ionospheres with the indicated range of hmF2 and x, is consistent with single-hop modes propagating to greater distances for lower layer heights, and also for lower x-values with significant refraction below the F2-region. For comparison, the broken curve from Appleton and Beynon [11] applies for a single parabolic F-layer with hmF2 = 250 km and ymF2 = hmF2/3.5. It can be seen that as x increases $M(D)$ for the composite profile shown in Fig. 1 approaches values for a single parabolic layer: residual differences arise because the composite distribution incorporates a quasiparabolic form for the F2-layer. All curves have a maximum M value M_{max} (as given by eqn. 14) at a maximum range D_{max}.

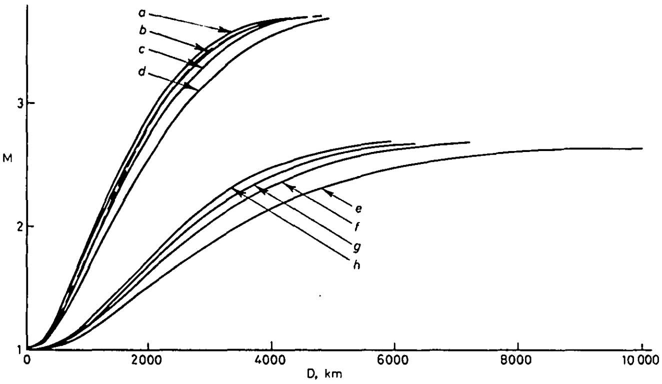

Fig. 3 *Variation of M-factors with range D for various x with hmF2 of 250 and 500 km*

– – – single parabolic layer with hmF2 of 250 km

hmF2 = 250 km	hmF2 = 500 km
a x = 10.0	e x = 2.0
b x = 3.3	f x = 2.5
c x = 2.5	g x = 3.3
d x = 2.0	h x = 10.0

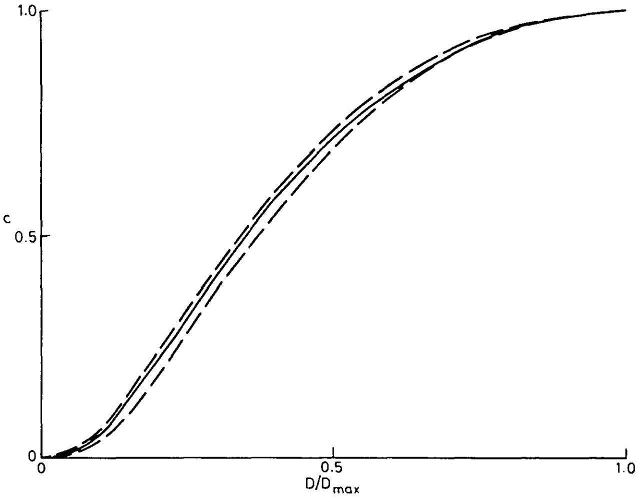

Fig. 4 *Variation of c (see eqn. 15 of text) with D as a ratio of the maximum value D_{max}*

—— polynomial fit given by eqns. 16 and 17

– – – extremes of variation of model cases

Fig. 4 shows the variation of a convenient parameter c, defined as

$$c = (M - 1)/(M_{max} - 1) \tag{15}$$

as a function of D/D_{max}. For all 42 cases the curves lie between the broken lines, and a simplified representation, giving a reasonable fit to all cases, is

$$c = c_D = 0.72 - 0.628z - 0.451z^2 - 0.03z^3 + 0.194z^4 + 0.158z^5 + 0.037z^6 \tag{16}$$

where

$$z = 1 - \frac{2D}{D_{max}} \tag{17}$$

which is shown by the solid line in Fig. 4. The values of D_{max} were calculated for each model profile from $\beta_0 = 0$ and $f = f_{max}$ and are shown as a function of $1/M(3000)_o$ for various x by the points of Fig. 5. Also plotted is a family of straight lines given by

$$D_{max} = 3940 + s\left\{\frac{1}{M(3000)_o} - 0.258\right\} \tag{18}$$

where D_{max} is in kilometres. It can be seen that, by adjusting the value of s, a reasonable fit to all points can be achieved. The error is largest for high hmF2 and low x, where the inverse proportionality of D_{max} and $M(3000)_o$ begins to break down. The values of s yielding a least-squares fit to the calculated points for each x are shown in Fig. 6. The solid curve is given by

$$s = 9900 + \frac{15375}{x^2} + \frac{106700}{x^5} \tag{19}$$

Eqns. 14–19 allow the development of algorithms for the simplified prediction of M-factor. This is done in two stages: in the following Section an algorithm is derived to estimate M

Table 1: Largest percentage errors in M-factors using eqns. 16–20

	x	hmF2					
		250 km	300 km	350 km	400 km	450 km	500 km
$D < 3000$ km	2.00	−3.8	−3.7	−4.0	−3.8	−3.2	−2.9
	2.08	−4.0	−3.7	−3.7	−3.5	−3.3	−3.1
	2.22	−4.5	−3.9	−4.2	−4.1	−3.6	−3.9
	2.50	−2.7	−2.0	−1.8	−1.1	−0.7	−0.3
	3.33	−3.1	−1.1	−0.4	0.4	0.9	1.5
	5.00	−3.3	−1.3	0.4	1.0	1.7	2.1
	10.00	−3.4	−0.8	0.6	1.4	1.9	2.6
$D > 3000$ km	2.00	−1.2	−1.7	1.7	2.8	3.2	6.0
	2.08	−1.7	−1.8	−2.5	−0.9	1.8	3.1
	2.22	−2.6	−2.8	−3.0	−0.8	0.5	1.6
	2.50	−0.5	−0.7	−1.2	−0.8	−0.5	0.9
	3.33	−0.3	−0.4	−0.5	−1.1	−1.4	−1.0
	5.00	−0.4	−0.5	−0.7	−1.3	−0.9	−1.6
	10.00	−0.6	−0.7	−0.8	−0.9	−1.1	−1.5

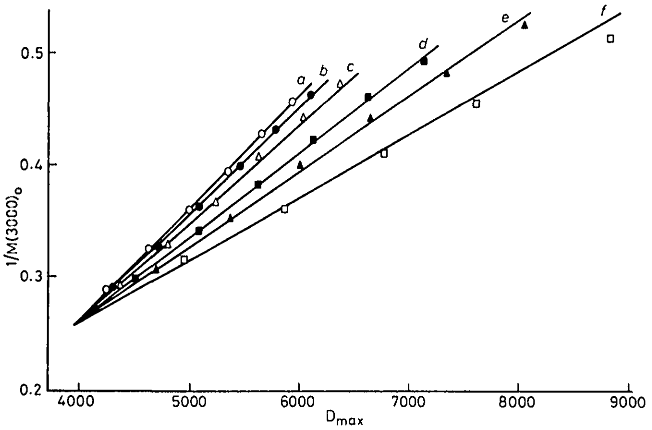

Fig. 5 *Maximum range D_{max} as a function of the inverse of $M(3000)_o$ for various x*

a $x = 10.0$ *d* $x = 2.5$
b $x = 5.0$ *e* $x = 2.2$
c $x = 3.3$ *f* $x = 2.0$

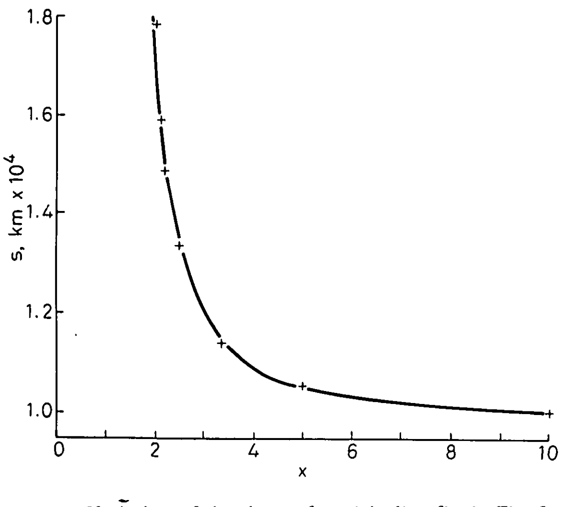

Fig. 6 *Variation of the slope of straight-line fits in Fig. 5, s, with x*

at a range D in terms of a known value at 3000 km, $M(3000)_o$; then in Section 6 the calculation of $M(3000)_o$ from ionogram data is considered. Eqns. 16–18 are approximate fits to the full calculations, and the errors they introduce will also be discussed.

5 Calculation of the M-factor at a range D from a known value at 3000 km

Eqns. 14–19 enable $M(D)$ to be calculated in terms of x, $M(3000)_o$ and hmF2. The value of x can be derived easily from an ionogram; however, hmF2 is not readily available, nor has it been mapped globally for prediction purposes. Hence it is desirable to avoid the requirement to know the value of hmF2. In addition the errors in making polynomial fits to the full calculations will cause the predicted value of M for $D = 3000$ km to differ in general from the known correct value of $M(3000)_o$ by some error. These two problems have a common solution which is demonstrated in Fig. 7.

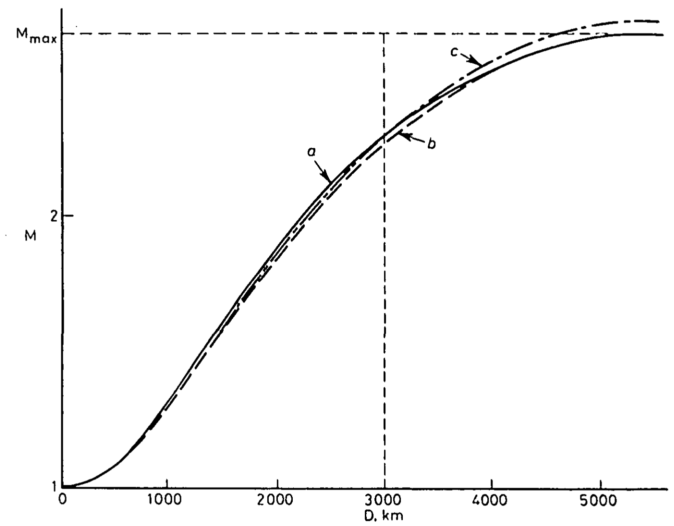

Fig. 7 *Variation of M-factors with range D*

a Full calculations M_T
b Polynomial fit
c Polynomial fit normalised at 3000 km M_p

The solid curve a shows the variation of fully calculated M-factors for the example hmF2 = 500 km and $x = 10$, and the broken curve b is the approximate fit from eqns. 14–19, the error at $D = 3000$ km being relatively large for this particular case. The curve c is given by

$$M = 1 + \left\{\frac{c_D}{c_{3000}}\right\}(M(3000)_o - 1) \tag{20}$$

where c_D and c_{3000} are given by eqns. 16 and 17 for ranges D and 3000 km, respectively. The normalising factor (c_D/c_{3000}) is chosen so that, by eqn. 20, curve c intersects curve a at $D = 3000$ km, giving zero error at that distance. Hence eqns. 16–20 allow $M(D)$ to be calculated from x and $M(3000)_o$.

It can be seen from Fig. 7 that improved fit of curve a near $D = 3000$ km is achieved at the expense of an increased error at the greatest ranges. The percentage error ξ was calculated as a function of range for each of the 42 profiles analysed ξ

being defined as

$$\xi = \left\{\frac{M_p - M_T}{M_T}\right\} 100 \qquad (21)$$

where M_p is calculated from eqns. 16–20, and M_T is the value from the full calculations for that range. Hence positive values of ξ represent over estimates of the M value. Fig. 8 shows ξ as a function of D for hmF2 of 350 km and various x. The error is always zero when D is zero ($M = 1$) and 3000 km, because of the normalisation introduced by eqn. 20. For low x the tendency is to underestimate M at ranges less than 3000 km and overestimate at the greater ranges. The errors are smaller at higher x. Table 1 gives the maximum error in the ranges $D < 3000$ km and $D > 3000$ km for each of the 42 profiles. The largest of these values is 6% for hmF2 = 500 km and $x = 2$, but this error occurs at $D = 8000$ km, a distance for which a single-hop MUF prediction is of limited practical application. For the larger ranges the combination of high hmF2 and low x always gives the greatest errors. The error maxima occurring at ranges near 1000 km are up to 4%. There is a tendency to underestimate M (negative ξ) except at high x and high hmF2 for $D < 3000$ km and at low x and high hmF2 for $D > 3000$ km. For both short- and long-distance paths the estimates of M for a particular hmF2 are least accurate for low x.

6 *M*(3000) scaled from ionograms

The preceding Section allows the calculation of M at any range, given the value for 3000 km. In practice the only estimates of this value available come from ionograms scaled using the standard URSI slider [3]. This slider is based on a constant correction factor of 1.115 for ionosphere and earth curvature in the vertical to oblique transformation, a value which must be an approximation for all but one case [12]. Hence $M(3000)_i$, the value scaled from ionograms, does not, in general, equal the M-factor calculated using the Milsom equations, $M(3000)_o$. To calculate $M(3000)_i$ for 42 profiles it is necessary to synthesise the ionogram corresponding to each of them.

The group height G was calculated as a function of f for $\beta_0 = \pi/2$. In general the segment of the ray path between r_b and r_t (see Fig. 2) makes a contribution J to the total group path, given by

$$J = \int_{r_b}^{r_t} \frac{r\,dr}{\{r^2\mu^2(r) - R_E^2\cos^2\beta_0\}} \qquad (22)$$

which can be solved for each of the segments of the profile, giving the total group path for the F-layer mode:

$$G = 2(J_1 + J_2 + J_3 + J_4) \qquad (23)$$

where

$$J_1 = r_{bE}\sin\gamma - R_E\sin\beta_0 \qquad (24)$$

$$J_2 = \frac{(Ar_{mE}^2 + Br_{mE} + C)^{1/2}}{A} - \frac{r_{bE}\sin\gamma}{A} - \frac{B}{A^{3/2}}\left[\sinh^{-1}\left\{\frac{2Ar_{mE} + B_1}{(4AC - B^2)^{1/2}}\right\} - \sinh^{-1}\left\{\frac{2Ar_{bE} + B}{(4AC - B^2)^{1/2}}\right\}\right] \qquad (25)$$

$$J_3 = \frac{1}{2(-A_1)^{1/2}}\left[\sin^{-1}\left\{\frac{2A_1r_{mE}^2 + B_1}{(B_1^2 - 4A_1C_1)^{1/2}}\right\} - \sin^{-1}\left\{\frac{2A_1r_1^2 + B_1}{(B_1^2 - 4A_1C_1)^{1/2}}\right\}\right] \qquad (26)$$

$$J_4 = \frac{B_{11}}{2A_{11}^{3/2}}\log_n\left\{\frac{-(B_{11}^2 - 4A_{11}C_{11})^{1/2}}{2A_{11}^{1/2}(A_{11}r_1^2 + B_{11}r_1 + C_{11}) + 2A_{11}r_1 + B_{11}}\right\} - \frac{(A_{11}r_1^2 + B_{11}r + C_{11})^{1/2}}{A_{11}} \qquad (27)$$

The standard URSI slider was then applied to the synthesised ionogram in the usual way to give the value $M(3000)_i$.

The percentage errors in $M(3000)$, as scaled from ionograms, deduced by comparison with the ray-tracing results, are tabulated in Table 2 for the 42 model profiles; positive values are overestimates. For hmF2 between 300 km and 400 km the errors in Table 2 have the opposite sense to those in Table 1; hence errors in the estimates of $M(D)$ derived from ionograms in the manner proposed here tend to cancel. For the range of peak heights below 400 km the procedure for $M(D)$, used with an input value of $M(3000)_i$, is accurate to about 5%. However, errors at greater peak heights are up to 15% for large distances and low x.

The differences between $M(3000)_o$ and $M(3000)_i$ are plotted in Fig. 9 as a function of the square of $M(3000)_i$. The family of straight lines fitted to these points are generated by the function

$$M(3000)_o = M(3000)_i - 0.124 + (M(3000)_i^2 - 4)\left(0.0215 + 0.005\sin\left\{\frac{7.854}{x} - 1.9635\right\}\right) \qquad (28)$$

Table 3 gives the errors in $M(3000)_o$ values calculated by this equation from the $M(3000)_i$ values, the largest being 0.6%. Use of this equation to correct standard $M(3000)$ values from ionograms therefore reduces the maximum error by a factor of about ten.

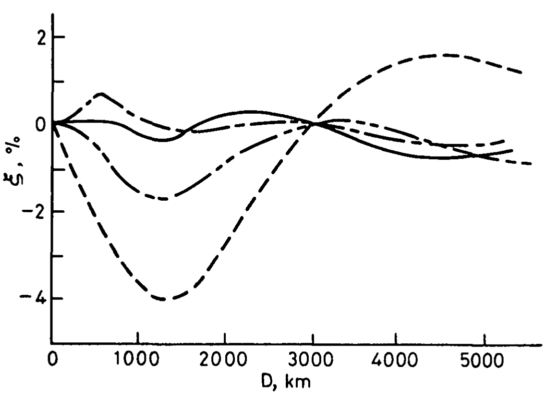

Fig. 8 *Percentage error ξ in predicted M value M_p as a function of range for various x*
--- $x = 2.0$
—-·-— $x = 2.5$
——— $x = 3.3$
—·— $x = 10.0$

Table 2: Percentage error in $M(3000)$ using URSI slider

x	hmF2					
	250 km	300 km	350 km	400 km	450 km	500 km
2.00	−1.5	1.5	2.8	4.5	5.7	7.5
2.08	−1.7	1.3	2.7	4.0	5.2	5.9
2.22	−1.7	0.5	2.4	3.6	4.8	5.7
2.50	−1.7	0.3	1.6	3.1	4.4	5.0
3.33	−1.2	0.2	1.6	2.7	3.8	4.7
5.00	−0.5	0.7	1.8	2.8	3.4	4.3
10.00	−0.2	1.0	2.1	3.0	3.8	4.3

7 Effect of geomagnetic field

All the equations of the preceding Sections have been based on the Milsom equations, which evaluate ray-path parameters neglecting the earth's magnetic field. Allowing for the effect of the field on propagation to 2000 km via a Chapman layer, Kopka and Moller [13] found the ordinary-wave MUF to be smaller, and the extraordinary-wave MUF to be larger, than the no-field value, the differences between these values depending on the path latitude, direction and length and on foF2. A simple correction to the field-free MUF, allowing for the extraordinary mode, is to add a fraction of the gyro-frequency, pf_H [14]; CCIR Report 340-4 adopts $p = 0.5$ for $D = 0$ and $p = 0$ and $D = 4000$ km. Considering this crude correction, a suitably simple corresponding expression for the extraordinary wave M-factor for $D \leqslant 4000$ km is

$$M_x = M\left(1 + \frac{f_H}{2f\mathrm{oF2}}\left\{1 - \frac{D}{4000}\right\}\right) \tag{29}$$

where D is in km and M is the no-field value given by eqn. 20.

8 Algorithm for M-factor prediction

Values of foE, foF2 and $M(3000)_i$ are available both from ionograms and from world maps [4]. Eqn. (28) allows the F2-layer $M(3000)$-factor to be corrected using the x value. The M-factor for F2-layer propagation to any range can then be calculated, neglecting the geomagnetic field, from eqns.

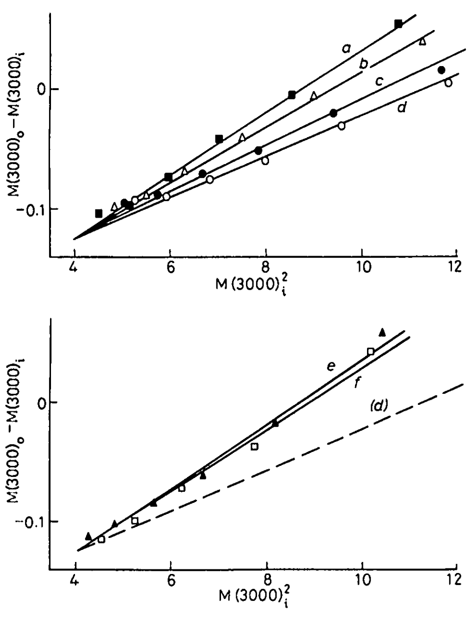

Fig. 9 *Difference between fully calculated M(3000)-factor and the value scaled from the vertical ionogram, $M(3000)_o - M(3000)_i$, as a function of the square of $M(3000)_i$*

a $x = 2.5$ *d* $x = 10.0$
b $x = 3.3$ *e* $x = 2.2$
c $x = 5.0$ *f* $x = 2.0$
– – – $x = 10$ for comparison with *e* and *f*

Table 3: Percentage error in $M(3000)$ using URSI slider with correction factor applied

x	hmF2					
	250 km	300 km	350 km	400 km	450 km	500 km
2.00	0.6	−0.5	−0.1	−0.3	0.2	−0.1
2.08	0.3	−0.6	−0.3	0.2	0.6	0.5
2.22	0.4	0.0	0.0	0.1	0.0	0.3
2.50	0.1	0.0	0.1	0.0	0.0	0.5
3.33	−0.2	0.0	0.0	0.1	0.1	0.2
5.00	−0.3	−0.1	0.0	0.1	0.5	0.5
10.00	0.1	0.1	−0.1	0.1	0.2	0.5

16–20, and correction can be made to allow for the extraordinary mode using eqn. 29.

In computerising the F-layer algorithm much of the code required is for eqn. 16. For E-layer modes it was found that to within an accuracy of 2% the single $M(D)$-factor curve could be described by eqn. 16 with the addition of a simple term, enabling calculation with very little extra computer store requirement:

$$c_E = c_D + 0.08 \sin\left[\pi\left\{\frac{D}{D_{max}}\right\}^{1/2}\right] \tag{30}$$

E-layer M-factor can then be calculated from eqns. 15, 16 and 30, as M_{max} equals 5.45 and D_{max} is 2750 km.

A standard Fortran subroutine, which calculates the larger of the E- and F-layer M-factors, is available on request from the author. The evaluation is performed in 12 lines of code with three calls of a nonlibrary function of two statements.

9 Conclusions

The use of Milsom's approximation to the Bradley-Dudeney model ionospheric profile enables rapid evaluation of M-factors for HF propagation via a spherically symmetric ionosphere, neglecting the effects on ray paths of the geomagnetic field and of electronic collisions. From these results a method for simple, rapid and accurate prediction of the basic maximum usable frequency has been devised. The algorithm is concise and requires an input of three ionospheric parameters for the centre of the hop: the critical frequencies for the E- and F-layers, and the $M(3000)$F2-factor as scaled from ionograms using the standard procedure and as stored in world maps.

The $M(3000)$F2-factor scaled using the standard URSI slider is found to differ from the results of full calculations by up to 7.5% for F2 peak heights less than 500 km, this maximum error falling to 3% for hmF2 below 350 km. The ratio of the critical frequencies can be used to correct the $M(3000)$F2-factor scaled from the ionogram so that it is always accurate to within 0.5%.

Using the corrected value for $M(3000)$F2 the algorithm calculates the M-factor for any required range to about 6%. The largest errors occur for ranges in excess of 4000 km, for which any method based on horizontal stratification is of limited use. For ranges less than 4000 km the algorithm developed here is accurate to within about 4%, which compares favourably with the likely accuracy of the ionospheric input data.

10 Acknowledgments

This work was carried out at the Rutherford Appleton Laboratory of the UK Science & Engineering Research Council as part of the Departmental Users Radio Propagation Programme. The author wishes to thank P.A. Bradley, who suggested the investigation and provided useful discussions.

11 References

1 'Definitions of maximum transmission frequencies'. CCIR Recommendation 373–4, 1982

2 'Second CCIR computer-based interim method for estimating sky-wave field strength and transmission loss at frequencies between 2 and 30 MHz'. Supplement to CCIR Report 252-2, 1978

3 PIGGOTT, W.R., and RAWER, K.: 'URSI handbook of ionogram interpretation and reduction'. US Department of Commerce, National Oceanic & Atmospheric Administration Report UAG-23, 1972

4 'CCIR atlas of ionospheric characteristics'. CCIR Report 340–4, 1982

5 BRADLEY, P.A., and DUDENEY, J.R.: 'A simple model of the vertical distribution of electron concentration in the ionosphere', *J. Atmos. Terr. Phys.*, 1973, **35**, pp. 2131–2141

6 DE VOOGT, A.H.: 'The calculation of the path of a radio ray in a given ionosphere', *Proc. Inst. Rad. Eng.*, 1953, **41**, pp. 1183–1186

7 CROFT, T.A., and HOOGASIAN, H.: 'Exact ray calculations in a quasi-parabolic ionosphere with no magnetic field', *Radio Sci.*, 1968, **3**, (1), pp. 69–74

8 MULDREW, D.B.: 'An ionospheric ray-tracing technique and its application to a problem in long distance radio propagation', *IRE Trans.*, 1959, **AP-7**, pp. 393–396

9 WESTOVER, D.E.: 'Exact ray path solutions for a quasi-linear ionosphere', *Radio Sci.*, 1968, **3**, (1), pp. 75–79

10 MILSOM, J.D.: 'Exact ray-tracing through the Bradley-Dudeney model ionosphere', *Marconi Rev.*, 1970, **40**, pp. 172–196

11 APPLETON, E.V., and BEYNON, W.J.G.: 'The application of ionospheric data to radio communication problems, Part 2', *Proc. Phys. Soc.*, 1947, **59**, p. 58

12 BRADLEY, P.A.: 'Computer procedure for deriving ionospheric characteristic *M*(3000)F2 from *h'*(*f*) data', *Electron. Lett.*, 1974, **10**, (15), pp. 323–324

13 KOPKA, H., and MOLLER, H.G.: 'MUF calculations including the effect of the Earth's magnetic field', *Radio Sci.*, 1968, **3**, (1), pp. 53–56

14 TREMELLEN, K.W., and COX, J.W.: 'The influence of wave propagation on the planning of short-wave propagation', *Proc. IEE*, 1947, **94**, (3A), pp. 200–219